

# Bose-Einstein condensation and Berezinskii-Kousterlitz-Thouless transition in 2D Nonlinear Schrödinger model

Sergey Nazarenko

*Mathematics Institute, The University of Warwick,  
Coventry, CV4-7AL, United Kingdom*

Miguel Onorato

*Dipartimento di Fisica, Università di Torino,  
Via Pietro Giuria 1, 10125 Torino, Italy and  
INFN, Sezione di Torino, Via Pietro Giuria 1, 10125 Torino, Italy*

Davide Proment\*

*School of Mathematics, University of East Anglia,  
Norwich Research Park, Norwich, NR4 7TJ, United Kingdom*

(Dated: June 8, 2022)

## Abstract

We analyse the Bose-Einstein condensation process and the Berezinskii-Kousterlitz-Thouless phase transition within the Gross-Pitaevskii model and their interplay with wave turbulence theory. By using numerical experiments we study how the condensate fraction and the first order correlation function behave with respect to the mass, the energy and the size of the system. By relating the free-particle energy to the temperature we are able to estimate the Berezinskii-Kousterlitz-Thouless transition temperature. Below this transition we observe that for a fixed temperature the superfluid fraction appears to be size-independent leading to a power-law dependence of the condensate fraction with respect to the system size.

---

\* [davideproment\[at\]gmail.com](mailto:davideproment@gmail.com); <http://www.uea.ac.uk/~xne12yku/>

## I. INTRODUCTION

When the lowest energy state of a Bose system becomes macroscopically occupied, that is to say a significant part of the total number of bosons are in that state, a Bose-Einstein condensate is said to emerge [1]. Usually this phenomenon manifests itself under a critical temperature called Bose-Einstein condensation temperature.

In an infinite homogeneous system the condensation depends strongly on the dimensionality. Indeed, in three dimensions the condensate is thermally stable while in less dimensions thermal fluctuations are strong enough to upset the long-range order. This is commonly known as Mermin-Wagner theorem [2] and it is due to the large-scale Goldstone modes (phonons), which have diverging infrared contributions to the particle density in one and two dimensions [3]. However, the long-range order can be restored in a finite system as the thermal fluctuations have an intrinsic cut-off at large scales [1]. Moreover, in 2D systems of interacting bosons another fascinating phase transition takes place. It is known as Berezinskii-Kosterlitz-Thouless (BKT) transition after the physicists who discovered it in the early 1970s, and it predicts that below a certain critical temperature  $T_{BKT}$ , the field correlations become “long” - decaying as a power law as opposite to the exponential decay law at higher temperatures [4–6].

There exist many links between processes in classical fluid turbulence and in wave turbulence to the Bose-Einstein condensation phenomenon [7–21]. It was understood that interacting Bose systems have features similar to fluids, vortices and waves, and that they can undergo a chaotic dynamics similar to turbulence. Then, condensation can be interpreted as an analogue of an inverse energy cascade in 2D fluid turbulence or an inverse cascade of waveaction in wave turbulence or the dissipative mechanisms carry a direct cascade may be used as prototypes of evaporative cooling.

Wave properties were also exploited for qualitative derivations of the algebraic decay of correlations in 2D interacting boson systems (acoustic modes - Bogoliubov phonons) and in explaining the BKT transition (vortices). A good recent review describing physical ideas and approaches in this area is given in Ref [22]. However, much of the physical picture remains elusive from the point of view of understanding fundamental wave and vortex dynamics responsible for these effects. A sophisticated renormalization group approach allows to formalise the statistical mechanics aspects of the problem and put them on a more solid

theoretical footing [23, 24], but it does not help clarifying the underlying wave and vortex dynamics and turbulence.

Moreover, the physical picture which is usually painted when describing the BKT transition remains oversimplified and unrealistic. It is said that the BKT transition occurs when the state changes from a gas of free hydrodynamic vortices at  $T > T_{BKT}$  to a gas of tight vortex dipoles at  $T < T_{BKT}$ . But to derive an exponential decay of the field correlations for  $T > T_{BKT}$  one usually appeals to Rayleigh-Jeans distribution of a non-interacting Bose gas, which contradicts the picture of hydrodynamic vortices because the latter are strongly nonlinear structures. Similarly, to derive a power-law decay of the field correlations for  $T < T_{BKT}$  one often uses Rayleigh-Jeans distribution of Bogoliubov phonons abandoning any appeal to hydrodynamic vortex pairs. Adding to the confusion, the Bogoliubov phonons are considered to be disturbances of a hypothetical superfluid density rather than of a uniform condensate density (the former tends to a constant and the latter tends to zero in the infinite box limit). However, there is no clear definition of such a superfluid density and there is no physical picture why is it legitimate to consider acoustic waves (phonons) in a fluid with such a density.

The present paper is an attempt by specialists in fluid and wave turbulence to understand physical processes accompanying the BKT transition and the condensation in finite 2D systems and, if possible, find analogies and interpretations of these processes within the conceptual framework of turbulence. We chose an approach of a direct numerical simulation (DNS) of a universal model which is a classical object for both turbulence (including wave turbulence, superfluid turbulence and optical turbulence [8, 15, 20]) and for the condensed matter theory of the BKT transition. Namely we will simulate the two-dimensional (2D) defocusing Nonlinear Schrödinger (NLS) equation (1), also known as the Gross-Pitaevskii equation in the Bose-Einstein condensate community.

To keep our model simple, we will not introduce any stochastic forcing representing a thermal bath, allowing the particle interactions (even when they are weak) to do the job of driving the system to the equilibrium thermodynamic state. This aspect of our model makes it different from the one used in Ref [25] where an external thermal bath forcing was used. Our system will be finite dimensional with a cut-off in the momentum space, and the finite values of the temperature and the chemical potential will be determined by the initial values of the energy and the number of particles in the system. Similar 2D NLS system

was recently computed in Ref [21] where the main emphasis was on the weakly nonlinear regimes for which an interesting phenomenon of a self-induced cutoff was discovered. In the present paper, we will study in detail the strongly nonlinear regimes associated with the BKT transition and with onset of condensation.

## II. THE MODEL AND DEFINITIONS

Let us consider a system described by the 2D defocusing NLS equation

$$i\partial_t\psi(\mathbf{x}, t) + \nabla^2\psi(\mathbf{x}, t) - |\psi(\mathbf{x}, t)|^2\psi(\mathbf{x}, t) = 0, \quad \mathbf{x} \in \mathbb{R}^2, t \in \mathbb{R}, \quad \psi \in \mathbb{C}. \quad (1)$$

It conserves the total number of particles

$$N = \int |\psi|^2 d\mathbf{x}$$

and the total energy

$$E = E_2 + E_4, \quad \text{where} \quad E_2 = \int |\nabla\psi|^2 d\mathbf{x} \quad \text{and} \quad E_4 = \frac{1}{2} \int |\psi|^4 d\mathbf{x} \quad (2)$$

are the free-particle and the interaction energies respectively.

Let the system be in a double-periodic square box with side  $L$ . Define Fourier transform,

$$\hat{\psi}_{\mathbf{k}} = \frac{1}{L^2} \int_{box} \psi(\mathbf{x}) e^{-i\mathbf{k}\cdot\mathbf{x}} d\mathbf{x}, \quad (3)$$

so that

$$\psi(\mathbf{x}) = \sum_{\mathbf{k}} \hat{\psi}_{\mathbf{k}} e^{i\mathbf{k}\cdot\mathbf{x}}, \quad (4)$$

where wave vectors  $\mathbf{k}$  take values on a truncated 2D lattice,

$$\mathbf{k} = \left( \frac{2\pi}{L} m_x, \frac{2\pi}{L} m_y \right), \quad m_x, m_y = -\frac{n}{2} + 1, -\frac{n}{2} + 2, -\frac{n}{2} + 3, \dots, \frac{n}{2}.$$

Note that truncation of the momentum (Fourier) space is essential for our considerations. Without such truncation we would face an “ultraviolet catastrophe”, i.e. the system would cool off to zero temperature no matter how much we would input energy in it initially. In real physical systems the role of such a momentum cut-off is played by the scale where the occupation number becomes of order one and the system is no longer described by a mean field model such as the NLS equation. Indeed, particles with higher momenta behave like a

classical Boltzmann gas with a rapidly decaying Maxwellian distribution - hence an effective cut-off momentum.

The mean density is

$$\bar{\rho} = \frac{1}{L^2} \int_{box} \langle |\psi(\mathbf{x})|^2 \rangle d\mathbf{x} = \sum_{\mathbf{k}} \langle |\hat{\psi}_{\mathbf{k}}|^2 \rangle, \quad (5)$$

Here, the angle bracket mean an ensemble average, whereas the overline means a double average - over the ensemble and over the box. Of course, because of the conservation of  $N$  the ensemble averaging in this formula is not necessary provided each realisation has the same number of particles. In this case  $\bar{\rho} = N/L^2$ . However, this averaging allows us to relate the density and the spectrum.

The spectrum is defined as follows,

$$n_{\mathbf{k}} = \frac{L^2}{(2\pi)^2} \langle |\hat{\psi}_{\mathbf{k}}|^2 \rangle, \quad (6)$$

The first order correlation function is

$$g_1(\mathbf{r}) = \langle \psi(\mathbf{0})\psi^*(\mathbf{r}) \rangle = \sum_{\mathbf{k}} \langle |\hat{\psi}_{\mathbf{k}}|^2 \rangle e^{i\mathbf{k}\cdot\mathbf{r}}; \quad \lim_{L \rightarrow \infty} g_1(\mathbf{r}) = \int n_{\mathbf{k}} e^{i\mathbf{k}\cdot\mathbf{r}} d\mathbf{k}. \quad (7)$$

Conversely, in the infinite box limit

$$n_{\mathbf{k}} = \frac{1}{(2\pi)^2} \int g_1(\mathbf{r}) e^{-i\mathbf{k}\cdot\mathbf{r}} d\mathbf{r}. \quad (8)$$

Relations between the mean density, the first-order correlation and the spectrum are function

$$\bar{\rho} = g_1(\mathbf{0}); \quad \lim_{L \rightarrow \infty} \bar{\rho} = \int n_{\mathbf{k}} d\mathbf{k}. \quad (9)$$

The spectrum at the zero mode is related with the first-order correlation function as follows,

$$n_0 = n_{\mathbf{k}=\mathbf{0}} = \frac{1}{(2\pi)^2} \int_{box} g_1(\mathbf{r}) d\mathbf{r}. \quad (10)$$

Given initial values of  $N$  and  $E$ , the system relaxes to its equilibrium state and may develop or not a macroscopic condensate fraction

$$C = \frac{n_0}{\sum_{\mathbf{k}} n_{\mathbf{k}}} = \frac{4\pi^2 n_0}{L^2 g_1(\mathbf{0})} = \rho_0 / \bar{\rho},$$

where  $\rho_0 = \langle |\psi_0|^2 \rangle = \langle |\hat{\psi}_{\mathbf{k}=\mathbf{0}}|^2 \rangle$  is the density of the particles in the zero momentum mode - the condensate density. Let us represent  $\psi$  as a sum of its box-averaged value and fluctuations,

$$\psi = \psi_0 + \tilde{\psi}; \quad \psi_0 = \frac{1}{L^2} \int_{box} \psi(\mathbf{x}) d\mathbf{x}$$

Now consider the Penrose-Onsager definition of the condensate density

$$\rho_c = g_1(\infty). \quad (11)$$

Easy to see that

$$\rho_c = \lim_{L \rightarrow \infty} \bar{\rho} \quad (12)$$

i.e.  $\rho_c$  is the condensate density in the infinite-box limit.

### III. WAVE TURBULENCE IN THE ABSENCE OF A CONDENSATE

For high temperatures, the gas is weakly interacting. In other words, for the typical wavenumber we have  $k^2 \gg \bar{\rho}$  and, therefore the nonlinear term is small compared to the linear term in the NLS equation (1). Such a small nonlinearity condition, together with an infinite box limit and an assumption of randomness, represent a standard setup of the wave turbulence (WT) approach, which allows to derive a four-wave kinetic equation [26]:

$$\dot{n}_k = 4\pi \int n_{\mathbf{k}_1} n_{\mathbf{k}_2} n_{\mathbf{k}_3} n_{\mathbf{k}} \left[ \frac{1}{n_{\mathbf{k}}} + \frac{1}{n_{\mathbf{k}_3}} - \frac{1}{n_{\mathbf{k}_1}} - \frac{1}{n_{\mathbf{k}_2}} \right] \times \delta(\omega_k + \omega_{k_3} - \omega_{k_1} - \omega_{k_2}) \delta(\mathbf{k} + \mathbf{k}_3 - \mathbf{k}_1 - \mathbf{k}_2) d\mathbf{k}_1 d\mathbf{k}_2 d\mathbf{k}_3. \quad (13)$$

where

$$\omega_k = k^2 \quad (14)$$

is the dispersion relation for the wave frequency.

In this four-wave WT regime, the leading effect of the weak nonlinearity (appearing at the lower order with respect to the energy transfers described by the kinetic equation (13)) is an upward nonlinear frequency shift [27] of the dispersion curve (14) by a  $\mathbf{k}$  independent value

$$\omega_{NL} = 2\bar{\rho}. \quad (15)$$

As we will see later, such a shift is easily detectable in numerical simulations, and its presence is a good indication that the system is in the four-wave condensate-free WT regime. Indeed, we will see that in presence of a strong condensate the frequency shift value at small wavenumbers is twice smaller.

A lot of WT studies focus on power-law spectra of Kolmogorov-Zakharov type which arise in forced and dissipated wave systems. However, there is no forcing or dissipation in

our finite-dimensional system, and a more relevant solution of the kinetic equation (13) in the steady state is given by the Rayleigh-Jeans distribution

$$n_{RJ}(\mathbf{k}) = \frac{T}{4\pi^2(k^2 + \mu)}, \quad (16)$$

where  $T$  and  $\mu$  are the temperature and the chemical potential of the system respectively. The free-particle energy density results in

$$\epsilon_2(T, \mu) \equiv E_2/L^2 = \int_{box} k^2 n_{RJ}(\mathbf{k}) d\mathbf{k} = \frac{T k_{max}^2}{\pi^2} - \mu \bar{\rho}. \quad (17)$$

Note that the interaction energy is small compared to the free-particle energy in this case, so the free-particle energy is approximately equal to the total (conserved) energy.

For the mean particle density we can write,

$$\bar{\rho}(T, \mu) = \int_{box} n_{RJ}(\mathbf{k}) d\mathbf{k} \approx \int_{k < 2k_{max}/\sqrt{\pi}} n_{RJ}(\mathbf{k}) d\mathbf{k} = \frac{T}{4\pi} \ln \left( 1 + \frac{4k_{max}^2}{\pi\mu} \right). \quad (18)$$

Here, to obtain the analytical expression we have replaced integration over the square box by integration within a circle of the same area which, although not absolutely precise, is quite accurate as we will see later.

Taking the inverse Fourier transform of the Rayleigh-Jeans distribution (16), we find asymptotically for large  $r$ ,

$$g_1(r) \approx \frac{\pi^{1/2} T}{(2r)^{1/2} \mu^{1/4}} e^{-\mu^{1/2} r}, \quad \text{for } r \gg \mu^{-1/2}, \quad (19)$$

which is the well-known result about the exponential decay of correlations in an uncondensed 2D weakly interacting (or non-interacting) Bose gas [22, 28].

#### IV. WAVE TURBULENCE IN PRESENCE OF A STRONG CONDENSATE

A different type of WT can be considered with a strong coherent condensate component

$$\Psi_0 = \sqrt{\rho_0} e^{-i\rho_0 t}, \quad \rho_0 = \text{const} > 0$$

(uniform in the physical space), and weak random disturbances  $\phi(\mathbf{x}, t)$  on the background of this condensate,

$$\psi(\mathbf{x}, t) = \Psi_0 (1 + \phi(\mathbf{x}, t)), \quad \phi \ll 1. \quad (20)$$

To develop the weak WT closure in this case, one has to diagonalize the linear part of the dynamical equation with respect to condensate perturbations  $\phi$ . Such a diagonalization procedure is called Bogoliubov transformation, which in the NLS case is as follows [7–9],

$$a_{\mathbf{k}} = \frac{\sqrt{\rho_0}}{2} \left[ \left( \frac{\omega_k^{1/2}}{k} - \frac{ik}{\omega_k^{1/2}} \right) \hat{\phi}_{\mathbf{k}} + \left( \frac{\omega_k^{1/2}}{k} + \frac{ik}{\omega_k^{1/2}} \right) \hat{\phi}_{-\mathbf{k}}^* \right], \quad (21)$$

or conversely

$$\hat{\phi}_{\mathbf{k}} = \frac{1}{2\sqrt{\rho_0}} \left[ \left( \frac{i\omega_k^{1/2}}{k} + \frac{k}{\omega_k^{1/2}} \right) a_{\mathbf{k}} - \left( \frac{i\omega_k^{1/2}}{k} - \frac{k}{\omega_k^{1/2}} \right) a_{-\mathbf{k}}^* \right], \quad (22)$$

where  $a_k$  are the new normal amplitudes, and  $\omega_k$  is the new frequency of the linear waves,

$$\omega_k = k\sqrt{k^2 + 2\rho_0}, \quad (23)$$

which is called the Bogoliubov dispersion relation [3]. Correspondingly, the relevant spectrum now is

$$n_{\mathbf{k}} = \frac{L^2}{(2\pi)^2} \langle |\hat{a}_{\mathbf{k}}|^2 \rangle. \quad (24)$$

For long waves,  $k^2 \ll \rho_0$ , the dispersion relation corresponds to acoustic waves - phonons,

$$\omega_k = c_s k, \quad c_s = \sqrt{2\rho_0}. \quad (25)$$

For short waves,  $k^2 \gg \rho_0$ , the dispersion relation is the same as for free particles,

$$\omega_k = k^2. \quad (26)$$

Now, the dominant nonlinearity is quadratic with respect to the condensate perturbations, and frequency (23) allows three-wave resonances. Thus, WT on background of a strong condensate is described by the standard three-wave kinetic equation,

$$\dot{n}_k = \int (\mathcal{R}_{\mathbf{k}_1\mathbf{k}_2}^{\mathbf{k}} - \mathcal{R}_{\mathbf{k}_1\mathbf{k}}^{\mathbf{k}_2} - \mathcal{R}_{\mathbf{k}\mathbf{k}_2}^{\mathbf{k}_1}) d\mathbf{k}_1 d\mathbf{k}_2, \quad (27)$$

where

$$\mathcal{R}_{\mathbf{k}_1\mathbf{k}_2}^{\mathbf{k}} = |V_{\mathbf{k}_1\mathbf{k}_2}^{\mathbf{k}}|^2 \delta(\omega_k - \omega_{k_1} - \omega_{k_2}) \delta(\mathbf{k} - \mathbf{k}_1 - \mathbf{k}_2) (n_{\mathbf{k}_1} n_{\mathbf{k}_2} - n_{\mathbf{k}_2} n_{\mathbf{k}} - n_{\mathbf{k}} n_{\mathbf{k}_1}) \quad (28)$$

with the following interaction coefficient [7–9],

$$V_{\mathbf{k}_1\mathbf{k}_2}^{\mathbf{k}_3} = \sqrt{\rho_0 \omega_{k_1} \omega_{k_2} \omega_{k_3}} \left[ \frac{6}{\sqrt{\alpha_{k_1} \alpha_{k_2} \alpha_{k_3}}} + \frac{1}{2} \left( \frac{\mathbf{k}_1 \cdot \mathbf{k}_2}{k_1 k_2 \alpha_{k_3}} + \frac{\mathbf{k}_2 \cdot \mathbf{k}_3}{k_2 k_3 \alpha_{k_1}} + \frac{\mathbf{k}_3 \cdot \mathbf{k}_1}{k_3 k_1 \alpha_{k_2}} \right) \right], \quad (29)$$



where  $\alpha_k = 2\rho_0 + k^2$ .

Rayleigh-Jeans equilibrium distribution now becomes

$$n_k = \frac{T}{4\pi^2\omega_k}. \quad (30)$$

Note that even for short waves,  $k^2 \gg \rho_0$ , the kinetic equation remains of the three-wave type as long as the fluctuations remain weaker than the condensate,  $\phi \ll 1$ . In this limit we get from (22)

$$\hat{\phi}_{\mathbf{k}} = \frac{(i+1)}{2\sqrt{\rho_0}} [a_{\mathbf{k}} - ia_{-\mathbf{k}}^*], \quad (31)$$

and assuming that waves with  $\mathbf{k}$  and with  $-\mathbf{k}$  have the same spectra but independent of each other phases,

$$\langle |\hat{a}_{\mathbf{k}}|^2 \rangle \approx \langle |\hat{\psi}_{\mathbf{k}}|^2 \rangle. \quad (32)$$

Thus, the Rayleigh-Jeans spectrum in this case is formally the same as the Rayleigh-Jeans spectrum for the four-wave (condensate free) system given by formula (16) with  $\mu = 0$ . This fact will be important for us for understanding the relation between the temperature  $T$  and the free-particle energy density  $\epsilon_2$ .

For long waves,  $k^2 \ll \rho_0$ , assuming that waves with  $\mathbf{k}$  and with  $-\mathbf{k}$  have the same spectra but independent of each other phases, we get from (22)

$$\langle |\hat{a}_{\mathbf{k}}|^2 \rangle \approx \frac{\sqrt{\rho_0/2}}{k} \langle |\hat{\psi}_{\mathbf{k}}|^2 \rangle. \quad (33)$$

In this limit the Rayleigh-Jeans distribution is

$$\langle |\hat{\psi}_{\mathbf{k}}|^2 \rangle \propto \frac{T}{k^2}. \quad (34)$$

This expression implies that at any finite  $T$  the integral of the number of particles is logarithmically divergent at  $k \rightarrow 0$  [3], which is a manifestation of absence of condensation in 2D NLS in an infinite system at any finite  $T$ . In the other words, our assumption that the fluctuations are weak compared to the condensate,  $|\phi| = |\tilde{\psi}/\Psi_0| \ll 1$ , fails in the equilibrium state in the infinite box limit, so that the Bogoliubov expansion around the condensate used in this section is inapplicable.

## V. HYDRODYNAMIC REFORMULATION AND POWER-LAW CORRELATIONS

We saw in the previous section that formal Bogoliubov expansion around a uniform condensate wavefunction  $\Psi_0$  fails in the equilibrium state. However, the way this expansion fails is quite revealing if we analyse the condensate disturbance  $\tilde{\psi}$  in the physical space. For waves which are much longer than  $\sqrt{\bar{\rho}}$  there is a complete equivalence of the NLS equation with the compressible hydrodynamics thanks to Madelung transformation

$$\psi = \sqrt{\rho} e^{i\theta}.$$

Interpreting  $\rho$  and  $\mathbf{u} = 2\nabla\theta$  as a fluid density and a fluid velocity respectively, we get the following equations of conservation of the fluid mass and the momentum respectively,

$$\frac{\partial\rho}{\partial t} + \nabla \cdot (\rho\mathbf{u}) = 0, \quad (35)$$

$$\frac{\partial\theta}{\partial t} + (\nabla\theta)^2 + \rho = 0. \quad (36)$$

For the acoustic waves around a uniform density  $\rho_0$ , the density and the velocity disturbances are related as

$$\frac{|\tilde{\rho}|}{\rho_0} = \frac{|\tilde{\mathbf{u}}|}{c_s} \equiv \frac{|\nabla\tilde{\theta}|}{\sqrt{2\rho_0}} \sim k \frac{|\tilde{\theta}|}{\sqrt{2\rho_0}}.$$

Thus, for long waves,  $k^2 \ll \rho_0$ , the fluctuations of the phase are much greater than the relative fluctuations of the density. Therefore, it is fluctuations of the phase and not the density that lead to violation of the condition  $|\phi| = |\tilde{\psi}/\Psi_0| \ll 1$  when  $\tilde{\theta} \sim 1$ .

On the other hand, the perturbation theory can be developed directly from the hydrodynamic equations (35) and (36) around a uniform state at rest  $\rho = \bar{\rho}$ ,  $\mathbf{u} = 0$ , in which case the approximation of weak nonlinearity is valid when  $|\mathbf{u}| \sim k|\tilde{\theta}| \ll c_s = \sqrt{2\bar{\rho}}$ , whereas changes in the phase itself can be of order one or even greater [28]. If the phase variations are strong, then even for nearly constant  $\rho$  we have  $\bar{\rho} \neq \rho_0$ . This state can be called a *quasi-condensate* because topologically it is equivalent to the true uniform condensate in a sense that there are no vortex-like phase defects in it.

Clearly, one can no longer use formulae (21) and (22) in this case, and the expression (34) will be invalid. Instead, one can obtain the correct relations from the energy written in terms of the hydrodynamic variables. In the limit  $k^2 \ll \bar{\rho}$  we have

$$E = E_2 + E_4 \approx \int \rho(\nabla\theta)^2 d\mathbf{x} + \frac{1}{2} \int \rho^2 d\mathbf{x}. \quad (37)$$

Correspondingly, for the wave energy we have in the leading order

$$\tilde{E} = \bar{\rho} \int (\nabla \tilde{\theta})^2 d\mathbf{x} + \frac{1}{2} \int \tilde{\rho}^2 d\mathbf{x}. \quad (38)$$

Here, the two terms have equal means by the virial theorem, so  $\tilde{E} = 2\bar{\rho} \int \langle (\nabla \tilde{\theta})^2 \rangle d\mathbf{x}$  or in Fourier representation

$$\tilde{E} = 2\bar{\rho} L^2 \sum_{\mathbf{k}} k^2 \langle |\hat{\theta}_{\mathbf{k}}|^2 \rangle.$$

Rayleigh-Jeans distribution is characterised by an energy equipartition in which each vibrational (phonon) mode has energy  $T$ ; this distribution becomes

$$\langle |\hat{\theta}_{\mathbf{k}}|^2 \rangle = \frac{T}{2\bar{\rho} L^2 k^2}. \quad (39)$$

Note that this is the same expression as the one which could be obtained from (30) in which  $a_{\mathbf{k}}$  is expressed using (22) and then the result is expressed in terms of the phase using expansion

$$\psi \approx \sqrt{\bar{\rho}} e^{i\theta} \approx \sqrt{\bar{\rho}} (1 + i\theta - \theta^2 + \dots)$$

However, now the result (39) goes beyond validity of such an expansion because  $\theta$  is no longer required to be small.

Let us now find the physical space correlation function  $g_1(\mathbf{r})$  for large  $r = |\mathbf{r}|$  taking into account that the main contribution to it will come from long-wave phonons with significant variations of  $\theta$  but negligible variations of  $\rho$ .

$$g_1(\mathbf{r}) = \langle \psi(\mathbf{0}) \psi^*(\mathbf{r}) \rangle \approx \bar{\rho} \langle e^{i(\theta(\mathbf{0}) - \theta(\mathbf{r}))} \rangle = \bar{\rho} e^{-\langle (\theta(\mathbf{0}) - \theta(\mathbf{r}))^2 \rangle / 2}, \quad (40)$$

where we assumed  $\theta$  to be a Gaussian random variable. In Fourier space we have

$$\langle (\theta(\mathbf{0}) - \theta(\mathbf{r}))^2 \rangle = \sum_{\mathbf{k}} |1 - e^{i\mathbf{k}\cdot\mathbf{r}}|^2 \langle |\hat{\theta}_{\mathbf{k}}|^2 \rangle = \frac{2T}{\bar{\rho} L^2} \sum_{\mathbf{k}} \frac{[\sin(\mathbf{k} \cdot \mathbf{r}/2)]^2}{k^2}.$$

Replacing in the large box limit the sum by an integral which is cut off at the end of the phonon range,  $k_{cut} \sim 1/\xi$ , where  $\xi = 1/\sqrt{\bar{\rho}}$  is the healing length, we have

$$\langle (\theta(\mathbf{0}) - \theta(\mathbf{r}))^2 \rangle \approx \frac{T}{2\pi^2 \bar{\rho}} \int_0^{1/\xi} \frac{[\sin(\mathbf{k} \cdot \mathbf{r}/2)]^2}{k^2} d\mathbf{k} \approx \frac{T}{2\pi \bar{\rho}} \ln(r/\xi), \quad \text{for } r \gg \xi.$$

Substituting this expression into equation (40), we finally obtain

$$g_1(r) = \bar{\rho} \left( \frac{\xi}{r} \right)^{1/(\lambda^2 \bar{\rho})}, \quad \text{for } r \gg \xi. \quad (41)$$

Here, we introduced notation for the thermal de Broglie length,

$$\lambda = \sqrt{\frac{4\pi}{T}}.$$

The law of algebraic decay of the correlations (41) is the central result in the statistical theory of 2D Bose systems.

As we can see, it is sufficiently rigorous and fully consistent with WT: it is rigorously valid as long as the density perturbations (phonons) remain weaker than the condensate density,  $\tilde{\rho} \ll \bar{\rho}$ , which is true for sufficiently low temperature. Moreover, under the same conditions one can use the three-wave WT kinetic equation (27) to describe evolution out of equilibrium (with  $\rho_0$  replaced by  $\bar{\rho}$ ).

On the other hand, for higher temperatures the density fluctuations grow and eventually become of the same order as the mean density,  $\tilde{\rho} \sim \bar{\rho}$ . Thus, even though the perturbation expansion based on the hydrodynamic formulation goes further than the one based on the original NLS, it still fails for larger  $T$ . The most intriguing development in the statistical theory of 2D Bose systems is the claim that law (41) is valid even in the infinite-box limit when  $\bar{\rho}$  is replaced by a (finite in the  $L \rightarrow \infty$  limit) *superfluid density*  $\rho_s$  [22]:

$$g_1(r) = \rho_s \left(\frac{\xi}{r}\right)^\alpha; \quad \alpha = \frac{1}{\lambda^2 \rho_s}. \quad (42)$$

Legitimacy of introducing such an effective density could be derived from the fact that of large density fluctuations the kinetic energy (the first term in (37)) is not equal to its constant density representation (the first term in (38)): rather it is greater than it via the Cauchy-Schwartz inequality. Such an imbalance could be phenomenologically corrected by replacing the constant density  $\bar{\rho}$  with a constant density  $\rho_s < \bar{\rho}$ :

$$E_2 = \int \rho (\nabla\theta)^2 d\mathbf{x} \approx \rho_s \int (\nabla\theta)^2 d\mathbf{x} < \bar{\rho} \int (\nabla\theta)^2 d\mathbf{x}. \quad (43)$$

Let us use this law to find a relation between  $\rho_s$  and  $\rho_0$ . Integrating expression (42), we have

$$\rho_0 = \frac{1}{L^2} \int_{box} g_1(\mathbf{r}) d\mathbf{r} = \frac{\rho_s}{L^2} \int_{box} \left(\frac{\xi}{r}\right)^\alpha d\mathbf{r} \approx \frac{2\pi\rho_s}{L^2} \int_{circle} \left(\frac{\xi}{r}\right)^\alpha r dr = \frac{2\pi^{\alpha/2}\rho_s}{(2-\alpha)} \left(\frac{\xi}{L}\right)^\alpha, \quad (44)$$

where we replaced integration over the square box by integration over the circle of the same area,  $r < L/\sqrt{\pi}$ .

Suppose that in the limit  $L \rightarrow \infty$  the value of  $\rho_s$  approaches a finite limit. Then, at fixed  $E$  and  $N$ , the condensate density  $\rho_0$  tends to zero as  $1/L^\alpha$ .

## VI. BKT TRANSITION

BKT transition is an effect of changing an exponential character of the correlation decay given by expression (19) to a power-law decay as in (42) when temperature drops below a critical value  $T = T_{BKT}$ .

First of all, without considering any physics one can claim that for the BKT transition to happen the nonlinearity (interaction) must fail to be weak in the 2D NLS system. Indeed, in weakly interacting systems the Rayleigh-Jeans distribution (16) is the only relevant equilibrium solution in the large box limit. One can take the ratio of the interaction and the free-particle energy densities,  $\sigma = \epsilon_4/\epsilon_2$ , as a measure of the interaction strength. We will see that  $\sigma(\rho, \epsilon_2)$  is indeed size-independent and that the BKT transition occurs almost precisely when  $\sigma = 0.5$ , i.e. then the nonlinear contributions are almost the same as the linear ones (recall that the contribution of  $\epsilon_4$  into the dynamical equation comes with weight 2 because of presence of two  $\psi^*$ 's in  $\epsilon_4$ ).

As we saw in the previous section, the power-law decay of correlations (42) at sufficiently low temperatures can be obtained systematically, although replacing  $\bar{\rho}$  with  $\rho_s$  when passing to the infinite-box limit is the least rigorous part in this approach.

However, the most striking prediction of the BKT theory is the value of the exponent of the power law just below  $T = T_{BKT}$ :

$$\alpha = \frac{1}{\lambda^2 \rho_s} = \frac{T_{BKT}}{4\pi \rho_s} = 1/4. \quad (45)$$

The standard physical argument leading to this prediction considers hydrodynamic vortices of radius  $\xi$  and single quantum of circulation  $\kappa = 4\pi$  in our dimensionless units (see eg. [22]). In a 2D box of size  $L$  the energy of a single quantum vortex is  $E_v \approx 2\pi\rho_s \ln(L/\xi)$  and its associated entropy is  $S \approx 2 \ln(L/\xi)$ , i.e. log of the maximum number of vortices that can be packed into the box of size  $L$ . Then the free energy of the system is

$$F = E_v - TS \approx \frac{T}{2}(\rho_s \lambda^2 - 4) \ln\left(\frac{L}{\xi}\right), \quad (46)$$

showing a change of sign at  $\rho_s \lambda^2 = 4$ , which corresponds to the BKT transition temperature and appearance of the power law with exponent (45). Below  $T = T_{BKT}$  we have  $F > 0$  so that formation of a new vortex is energetically unfavourable. It is usually said that tight vortex dipoles would be present in this case, with the number of such dipoles decreasing

when the system is cooled more. Above  $T = T_{BKT}$  we have  $F < 0$  so that formation of new vortices is energetically favourable and we should expect proliferation of vortices which results in a state with a “gas” of “free” (i.e. unbound) vortices.

It is not hard to see that the standard physical argument reproduced above is oversimplified, at least in the case of the 2D NLS system. Firstly, NLS vortices can only be viewed as hydrodynamic if the distance between the vortices is much greater than their radius (the healing length  $\xi$ ). This is not the case neither below nor above  $T_{BKT}$ . Moreover, the fact that at  $T = T_{BKT}$  the linear and the nonlinear energies are equal means that at this temperature the mean distance between the vortices is of order  $\xi$ , and that raising temperature further above  $T_{BKT}$  make the system more and more weakly nonlinear. In this case, the vortices are very dissimilar to their hydrodynamic counterparts - they are often called ghost vortices, because they do not have a dynamical significance being zeroes of a weakly nonlinear wave field whose spectrum is described by the four-wave kinetic equation (13). Later, we will also see that such dipoles are not the most typical vortex structures below  $T_{BKT}$  unless  $T$  is significantly less than  $T_{BKT}$ . These vortices are also insignificant for the observed dynamical and statistical properties below  $T_{BKT}$ : as we saw in the previous section the low-frequency phonons are much more important.

Keeping in mind these inconsistencies of the physical argument based on the hydrodynamical vortices which applied to the 2D NLS system, it appears to be even more striking that, as we will see later, its prediction for the critical exponent  $\alpha = 1/4$  appears to be accurate. This prediction at the BKT transition point is however a standard and rigorous result in statistical mechanics obtained using for example the XY model, which belongs to the same class of universality [6].

## VII. NUMERICAL RESULTS

We have performed series of direct numerical simulations (DNS) of the 2D NLS equation in a doubly periodic square box using a pseudo-spectral method. Our numerical code computes the integration in time using a split-step method, a standard technique for this model. We have tried several different values of the box size  $L$ . In all our simulations, both wavevector components  $k_x$  and  $k_y$  we truncated at the maximum absolute value of

$$k_{max} = \frac{n}{2} \frac{2\pi}{L} = \pi, \quad (47)$$

where  $n$  is the number of resolution point in both the  $x$ - and  $y$ -directions. This corresponds to an effective physical grid with spacing

$$\Delta x = \frac{2\pi}{2k_{max}} = 1, \quad (48)$$

so that  $n = L$ .

Our goal was to study thermodynamic equilibria, so there were no damping or forcing terms in our DNS. The initial conditions were chosen so that in all simulations the mean density was kept the same,  $\bar{\rho} = 1$ , and the energy took a range of different initial values. Initially we populated a fraction of high energy modes setting random phases and then we waited till a final equilibrium statistically steady state is reached driven by the nonlinear interactions.

The healing length  $\xi$  is defined so that the linear and the nonlinear terms in the NLS equation are approximately equal to each other,

$$\xi = \frac{1}{\sqrt{\bar{\rho}}} = 1. \quad (49)$$

Near its centre, the vortex solution behaves as  $\psi \approx 0.6(x + iy)$  using healing length units [29], so that the vortex core size  $a$  can be estimated as

$$a \approx \frac{\xi}{0.6} \approx 1.7 = 1.7 \Delta x. \quad (50)$$

Thus, each vortex is resolved by approximately  $\pi a^2 \approx 9$  grid points. For the corresponding wavenumber we have

$$k_a = \frac{1}{a} \approx 0.6 \approx k_{max}/5.2, \quad (51)$$

and in the low-temperature Bogoliubov regime we expect to see both the phonon range of scales,  $k < k_a$ , and “free particles” with  $k > k_a$ . In fact, in this regime most of the particles will be in the condensate mode ( $\mathbf{k} = 0$ ) and in the phonons, and most of the energy will be in the free particles (see further considerations and Fig. 10).

### A. Dispersion relation and the frequency shift

First of all, let us examine the wave properties of the system and compare them with the theoretical predictions for very high and for very low temperatures. For this, let us perform frequency Fourier transform of  $\hat{\psi}_{\mathbf{k}}(t)$  in the steady state over a sufficiently long window of

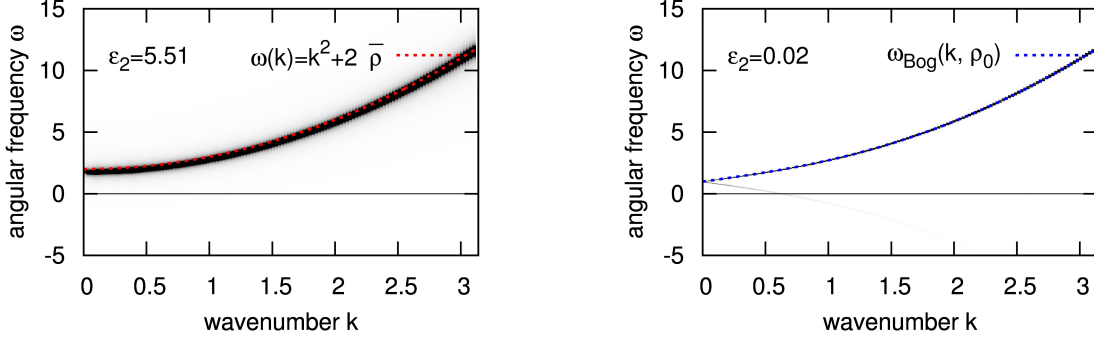


FIG. 1. (Color online) Dispersion relation in the presence of a weak (left) and a strong (right) condensate. Results are taken from simulations with  $L = 256$ .

time and plot the resulting spectrum  $|\hat{\psi}(\mathbf{k}, \omega)|^2$  on a 2D plot  $\omega$  vs  $k = |\mathbf{k}|$ . Representative examples of such plots are shown in Fig. 1: a case of high  $T$  on the left and a case of low  $T$  on the right respectively.

Our theoretical prediction for high temperatures is that the system is made of weakly interacting waves with the dispersion relation  $\omega_k = k^2 + \omega_{NL}$  with the frequency up-shift  $\omega_{NL}$  as in (15) and the spectrum obeying the four-wave kinetic equation (13). On the  $(k, \omega)$  plot such a weakly nonlinear system should manifest itself by a narrow distribution around curve  $\omega = \omega_k = k^2 + 2\bar{\rho}$ , as it is indeed seen in the left panel of Fig. 1. Note that the measured nonlinear shift  $\omega_{NL}$  is a little less than the theoretical  $2\bar{\rho}$ , which could be expected as this prediction is valid only when  $E_2 \gg E_4$ . For very low  $T$ , the theory predicts existence of two components - a strong condensate rotating with frequency  $\omega_0 = \rho_0 \approx \bar{\rho}$  and weakly interacting phonons with Bogoliubov dispersion law (23).

Note that this dispersion is for the normal variable  $a_{\mathbf{k}}$  whereas the Fourier transform of  $\psi$  should be shifted by the condensate frequency  $\omega_0$  and should have two branches corresponding to  $a_{\mathbf{k}}$  and  $a_{\mathbf{k}}^*$  respectively,

$$\omega_{Bog}(k) = \bar{\rho} \pm k\sqrt{k^2 + 2\bar{\rho}}.$$

Once again, we can see a very good agreement with these predictions on the right panel of Fig. 1. Indeed we see both phonon branches as well as the shift due to the condensate rotating frequency. Interestingly, we do not observe the horizontal line corresponding to a rotating non-uniform condensate state as previously observed in forced and damped NLS



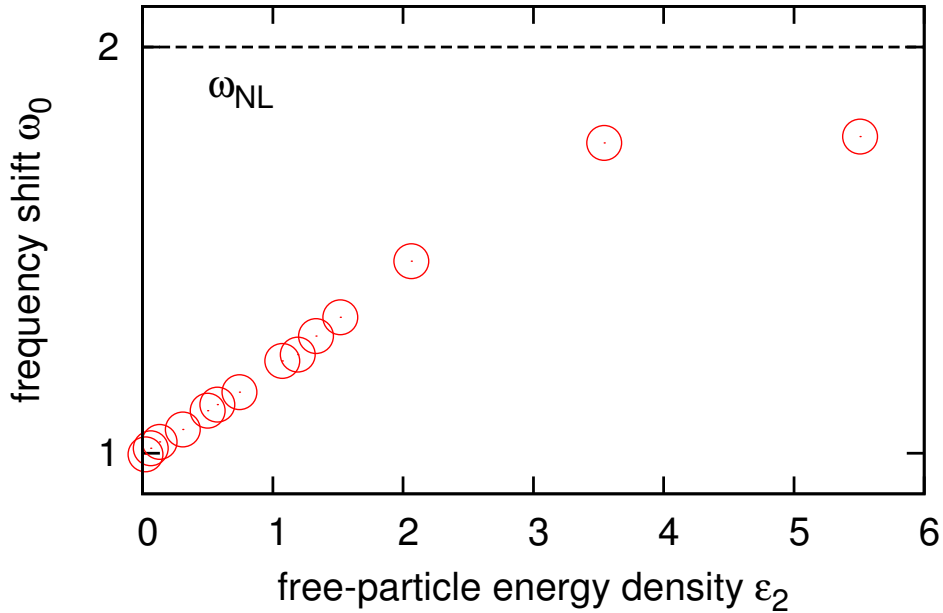


FIG. 2. (Color online) Measured frequency shift as a function of the free-particle energy  $\epsilon_2$ . Results taken from simulations with  $L = 256$ .

simulations [11, 12, 17]. This is an indicator that fully hydrodynamic vortices, making the condensate nonuniform and producing perturbations at  $k \neq 0$ , are absent in the equilibrium state, whereas such vortices were present in previous simulations which focused on non-equilibrium states.

What happens at the intermediate temperatures? This is the range where the classical wave turbulence based on weak nonlinearity expansions fails and where strong turbulence takes place characterised by a complex interplay of the vortex dynamics and strong acoustic pulsations. This is the range for which power-law correlations and the BKT transition were predicted based on phenomenological physical arguments presented in sections V and VI. There, the theory of Bogoliubov type was extended beyond its formal limits of applicability by introducing a hypothetical effective density - the superfluid density  $\rho_s < \bar{\rho}$ . But we are now in a position to test if replacing  $\bar{\rho}$  by  $\rho_s$  in the Bogoliubov theory, including the dispersion relation, would be a good approximation to reality. In particular we can examine the frequency shift  $\omega_0 = \omega_{k=0}$  on the  $(k, \omega)$  plots for the intermediate values of the temperature or, equivalently, intermediate values of the energy.

The result is shown in Fig. 2 as a plot of  $\omega_0$  as a function of free-energy density  $\epsilon_2$ .

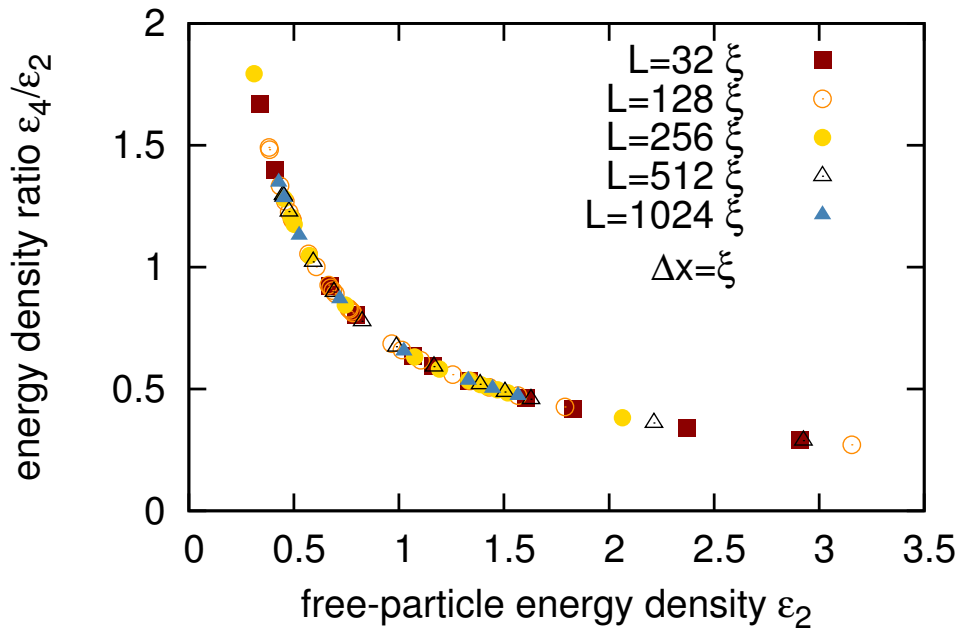


FIG. 3. (Color online) Steady-state ratio  $\epsilon_4/\epsilon_2$  as a function of  $\epsilon_2$ .

Here, we can see a monotonous increase of  $\omega_0$  as  $\epsilon_2$ , and therefore  $T$ , increase starting with the low- $T$  theoretical value of  $\bar{\rho}$  and aiming for another theoretical value  $2\bar{\rho}$  on the high- $T$  side. This is in clear disagreement with a naive replacement of  $\bar{\rho}$  by  $\rho_s$  in the Bogoliubov the dispersion relation, because this would give us  $\omega_0 = \rho_s$  which is a decreasing function of  $T$ . Thus, strong turbulence in the intermediate range of turbulence surrounding the BKT transition cannot be fully understood as Bogoliubov phonons on the background of an effective superfluid density.

### B. Identification of $T$ with $\epsilon_2$

First we will mention that for most experiments except to the ones with the highest energy we have  $T \approx \epsilon_2$ ; this will be justified later, see (52), but meanwhile, in the following subsections, this very useful fact will allow us to identify  $T$  with  $\epsilon_2$ .

### C. Strength of interactions

The interaction strength is a measure of the nonlinearity of the system. It can be quantified by the ratio of the interaction energy to the energy of the free particles,  $\sigma = \epsilon_4/\epsilon_2 = E_4/E_2$ , where  $E_2$  and  $E_4$  are defined in (2). Figure 3 shows the results for  $\sigma$  as a function of  $\epsilon_2$  in the steady state computed for  $\bar{\rho} = 1$  and different values of  $L$ . We see that the data for the different values of  $L$  collapse on the same curve, which implies that for fixed  $\epsilon_2$  and  $\bar{\rho} = 1$  the quantity  $\epsilon_4$  is  $L$ -independent. This is an interesting and nontrivial result considering the fact that the many other characteristics (eg. the condensate fraction, see next section) are  $L$ -dependent.

### D. Condensate fraction

Figure 4 shows the condensate fraction  $C = \rho_0/\bar{\rho}$  in the equilibrium state as a function of free-energy density  $\epsilon_2$  for systems having different sizes. One can see that  $C$  depends on the box size  $L$ : as could be expected it is greater for smaller  $L$ . Figure 5 shows  $C$  in the equilibrium state as a function of  $L$  at several different fixed values of  $\epsilon_2$  below the threshold. Note that  $\epsilon_2$  cannot be set *a priori*, therefore we considered values within an error of 5% in simulations having different  $L$ . We can see that  $C$  is a decreasing function of  $L$  which approximately follows the theoretically predicted power law (44).

Looking back at Fig. 4, we can appreciate that for large  $L$  the condensation threshold behaviour becomes more and more pronounced and the threshold value of  $\epsilon_2$  (and therefore of  $T$ ) tends to accumulate to a limiting value  $\epsilon_c \approx 1.4$  in the infinite-box limit. Of course, based on numerics alone it is impossible to conclude if such a limiting value exists or the threshold tends to zero very slowly as a function of  $L$ . Argument in favour of the finite threshold limit  $\epsilon_c$  was given before based on the view that for large  $L$  the condensation is interaction-induced and must occur when the nonlinearity degree  $\sigma$  reaches an order-one value. As we see in Fig. 3, the value of  $\sigma$  is  $\sim 0.5$  at  $\epsilon_2 = \epsilon_c \approx 1.4$  which means that the linear and nonlinear terms in the NLS equation balance (recall that the interaction energy contributes with factor 2 into the equation). In section VI we presented a similar argument that the BKT transition should be expected when  $\sigma$  reaches an order-one value. In fact, our numerics indicate that the condensation threshold temperature  $T_c \approx \epsilon_c \approx 1.4$  is very close

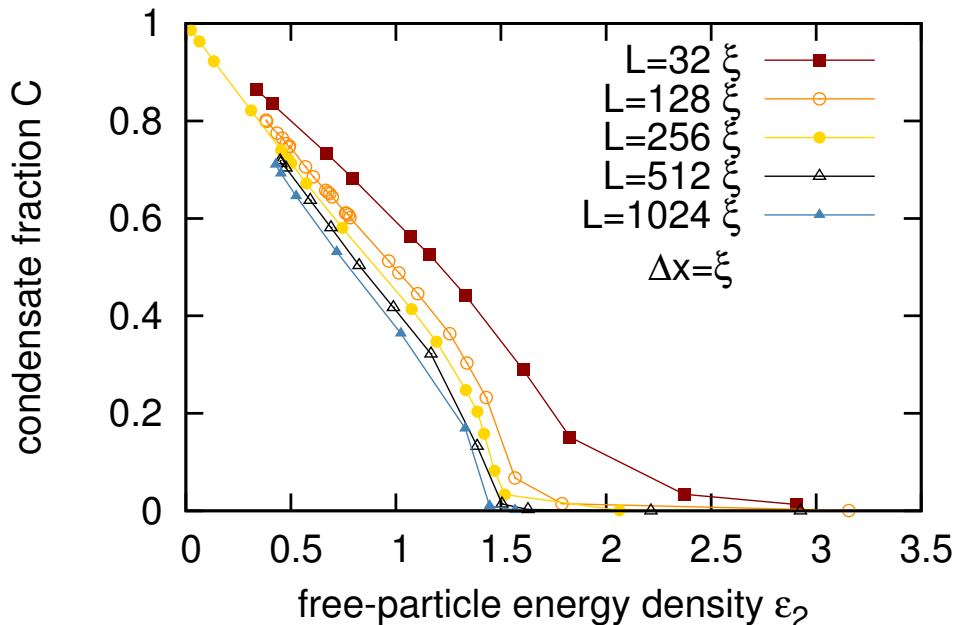


FIG. 4. (Color online) Steady-state condensate fraction  $C = \rho_0/\bar{\rho}$  as a function of the free-particle energy density  $\epsilon_2$ .

to the  $T_{BKT}$  or may be even equal to it.

Figure 5 shows the steady-state condensate fraction  $C = \rho_0/\bar{\rho}$  as a function of the box size  $L$  for different temperatures. We can see an excellent agreement with the predicted law (44). This result confirms the claim that the value of the superfluid density  $\rho_s$  is approximately  $L$ -independent. The value of  $\rho_s$  will be calculated for different temperatures in Fig. 8.

### E. Power-law correlations, superfluid density and BKT transition

At the BKT transition temperature  $T_{BKT}$  the first-order correlation  $g_1(r)$  is predicted to change from an exponential to a power-law decay, the former given in (19) and the latter in (42) respectively. In Fig. 6 we show a log-log plot of  $g_1(r)$  in simulations with  $L = 256$  with  $\bar{\rho} = 1$  and different values of the energy (i.e. corresponding to different temperatures). We see that indeed a power-law behaviour appears for  $T < T_{BKT} \approx 1.39$  (i.e. for  $\epsilon_2 < 1.39$ ). Note that this value is very close to the condensation threshold for large  $L$  which, as seen in Fig. 3, that is  $\epsilon_2 \approx 1.4$ . As we mentioned above, the nonlinearity degree  $\sigma$  has value  $\sim 0.5$  at this temperature, which corresponds to the balance of the linear and nonlinear

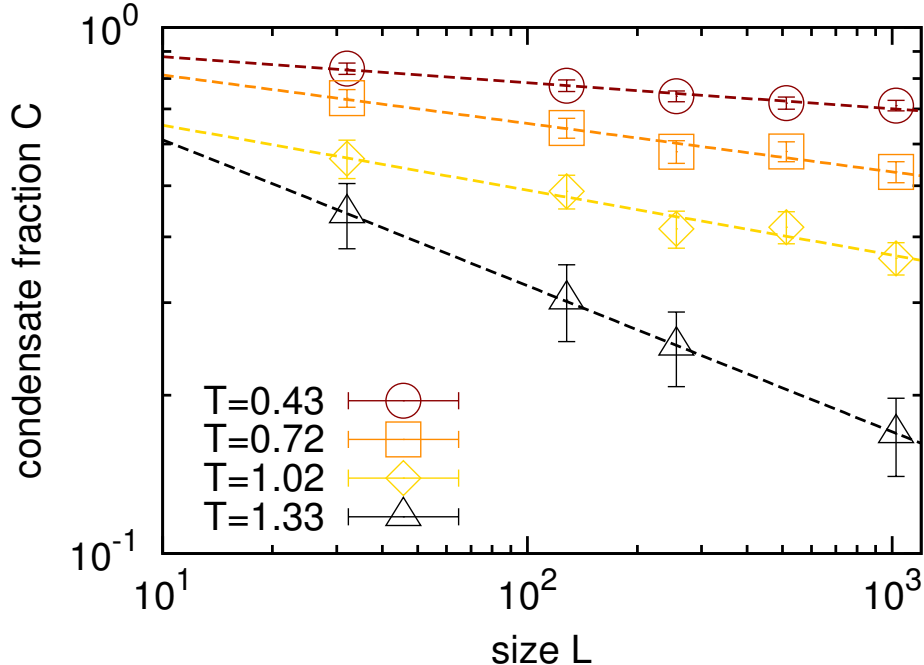


FIG. 5. (Color online) Steady-state condensate fraction  $C = \rho_0/\bar{\rho}$  as a function of the box size  $L$  for different temperatures. The straight dashed lines are best fits with the power law (44).

contributions in the NLS equation. This is different (although not by much) from the value  $T_{BKT} = 4\pi/\ln 760 \approx 1.89$  obtained in [30] by Monte Carlo simulations. One can see in Fig. 6 that the power-law exponent for temperatures just below  $T_{BKT}$  agrees very well with the predicted value  $\alpha = 1/4$ . This is especially amazing considering non-rigorous character of the physical argument based on the picture of hydrodynamic vortices. Indeed, as we mentioned in section VI and as we will discuss in detail below in subsection VII G the vortices in 2D NLS are never similar to their hydrodynamic counterparts at thermodynamic equilibria of any temperature - most of the time they lack nonlinearity to sustain themselves (ghost vortices) and they sporadically annihilate and get created before they get a chance to move hydrodynamically.

For the superfluid density we have from (44):

$$\rho_s \approx \frac{(2 - \alpha)}{2\pi^{\alpha/2}} \left(\frac{L}{\xi}\right)^\alpha \rho_0.$$

In particular, for  $L = 256$  and  $\xi \approx 1.7$  near the BKT transition,  $\alpha = 1/4$ , we have  $\rho_s \approx 2.6\rho_0$ . Reading the value of  $g_1(\xi) = \rho_s$  in Fig. 6 we get  $\rho_s \approx 0.62$ , so at the BKT transition point  $\rho_0 \approx 0.24$ . This value is in a reasonable agreement with the result for  $\rho_0/\bar{\rho} = \rho_0 \approx 0.17$  at

$T_{BKT} \approx 1.39$  in Fig. 4.

On the other hand, near the BKT transition we should have

$$\lambda^2 \rho_s = \frac{4\pi \rho_s}{T} = 4,$$

so the prediction is  $T_{BKT} = \pi \rho_s \approx 1.95$ , which is somewhat different from the value 1.39 obtained numerically. If we calculate based on the value  $T_{BKT} \approx \rho_0 \approx 0.17$  of Fig. 4, then we get a much better agreement,  $T_{BKT} = \pi 2.6 \rho_0 \approx \pi 2.6 \times 0.17 \approx 1.39$ . It is therefore reasonable to think that the true value of  $\rho_s$  at the BKT transition is around 0.5.

Actually, we are in the position to make measurements of  $\rho_s$  at different temperatures by equating the measured slopes on the log-log plots of  $g_1(r)$  with the value of  $\alpha$  in the second equation (42), ie.  $\alpha = T/(4\pi\rho_s)$ . For this, we first plot on Fig. 7 the log-log plots of  $g_1(r)$  for different  $T$  and  $L$ . We see that the resulting curves are nearly independent of  $L$  which confirm  $L$ -independence of  $\rho_s$ . Next, measuring slopes on these curves, we calculate  $\rho_s$  at different temperatures; the resulting dependence is shown in Fig. 8. In particular, we see that just below the BKT transition  $\rho_s \approx 0.38$ , which is in a reasonable agreement with our estimate in the previous paragraph.

Probably, the main factor contributing to (relatively minor) deviations of our results from the theoretical predictions is periodicity of our system because of which the correlation function  $g_1$  must be periodic and, clearly, expression (42) cannot be true for  $r \geq L/2$ .

## F. Spectra

Now we will consider the steady state spectra in simulations with  $L = 256$ ,  $\bar{\rho} = 1$  and different values of energy.

Figure 9 shows the spectra in simulations with high energies when no condensation is observed and the fits with Rayleigh-Jeans equilibrium distributions (16). One can see an excellent agreement between the data and the fits. Moreover, relation between the fits for  $T$  and  $\mu$  in Fig. 9 is in an excellent agreement with theoretical formula (18).

Figure 10 shows the spectra in simulations with low energies when a strong condensate is present, and it shows fits of these spectra by Rayleigh-Jeans equilibrium distributions (30). One can see a reasonable agreement between the data and the fits: this agreement is better for lower temperatures and stronger condensate, as could be expected. Also, these

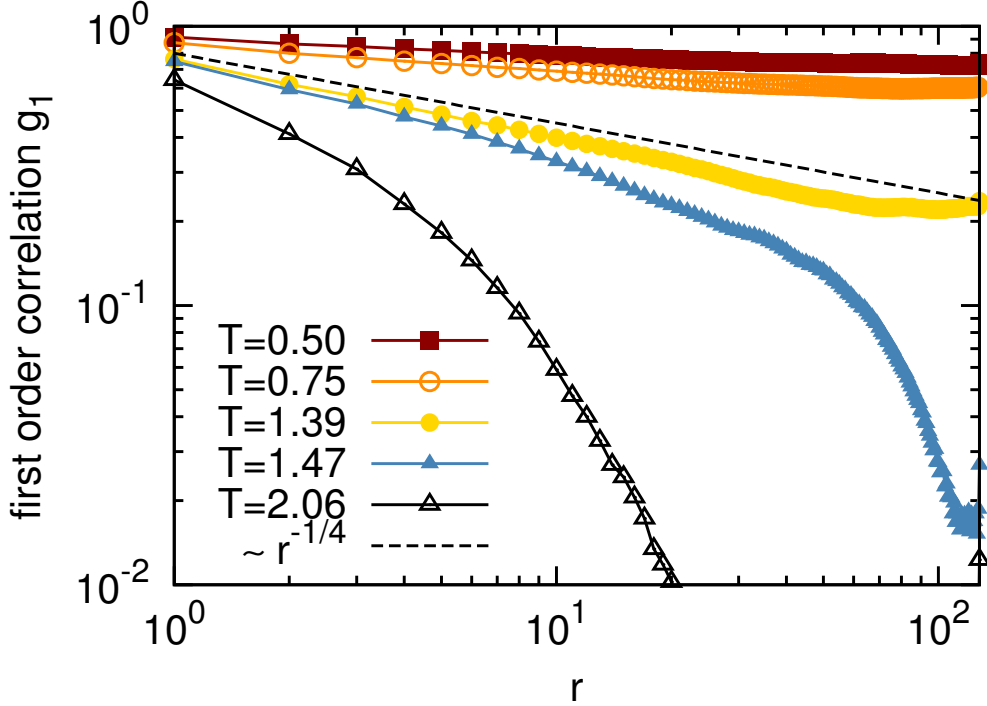


FIG. 6. (Color online) First-order correlation function of the field  $\psi$  for different values of linear energy. Results taken from simulations having side equal to  $L = 256$ .

fits get better in the range of higher  $k$ 's, which contains most of the systems energy, giving an advantage for a rather precise fit of  $T$ .

Figure 11 plots temperature  $T$ , obtained from the fits in Figs. 9 and 10, as a function of the free-particle energy  $\epsilon_2$ . Remarkably, for both the low- and the high-temperature ranges this plot is in an excellent agreement with the expression (17) for  $\epsilon_2$  in terms of  $T$  and  $\mu$ , which was theoretically obtained for the high-energy case. To understand why this expression works for the low-energy case, we first of all notice that in the low-energy case most energy comes from the range  $k > k_\xi = k_{max}/5.2$ . Indeed, since the energy in the thermodynamic state is equipartitioned over the 2D  $\mathbf{k}$ -space, the energy in the range  $k > k_\xi$  represents about 97% of the total energy. But in this range  $\omega_k \approx k^2$  and, according to formula (32), we have  $\langle |\hat{a}_{\mathbf{k}}|^2 \rangle \approx \langle |\hat{\psi}_{\mathbf{k}}|^2 \rangle$ . Thus, the RJ distribution in this range is the same as in for high-energy case with  $\mu = 0$ , see (16), and therefore expression (17) is also the same (with  $\mu = 0$ ).

Further, the second term on the RHS of expression (17), i.e. the one with  $\mu$ , is only important for very high temperatures. In particular, all data points on Fig. 11 except to

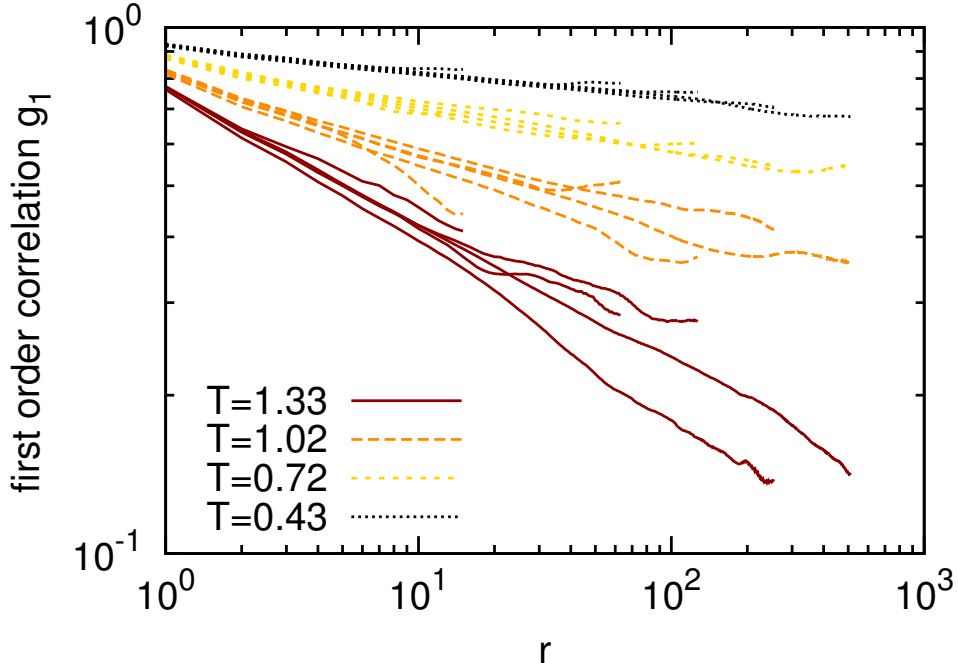


FIG. 7. (Color online) First-order correlation function of the field  $\psi$  for different values of temperatures below the estimated  $T_{BKT}$ . Equal coloured lines refer to simulations having the same temperature but different system size.

the one corresponding to the highest  $T$  fall onto line

$$T = \epsilon_2, \quad (52)$$

which is nothing but expression (17) without the second term on the RHS and with  $k_{max} = \pi$ . This is a remarkably simple expression which has allowed us to identify  $T$  and  $\epsilon_2$  in all of our numerical experiments (except for the highest  $T$ ).

### G. Vortices

Let us now look at the vortices, i.e. the zeroes of the field  $\psi$  where the phase changes by  $\pm 2\pi$ . It is well-known that NLS vortices behave similarly to hydrodynamic vortices if they are separated from each other by distances greater than the healing length  $\xi$ . For example, two vortices of the same sign would rotate around each other, two vortices of the opposite signs (a vortex dipole) would move along a straight line, etc. However, when vortex separations are less than  $\xi$  they behave very different from their hydrodynamic counterparts.



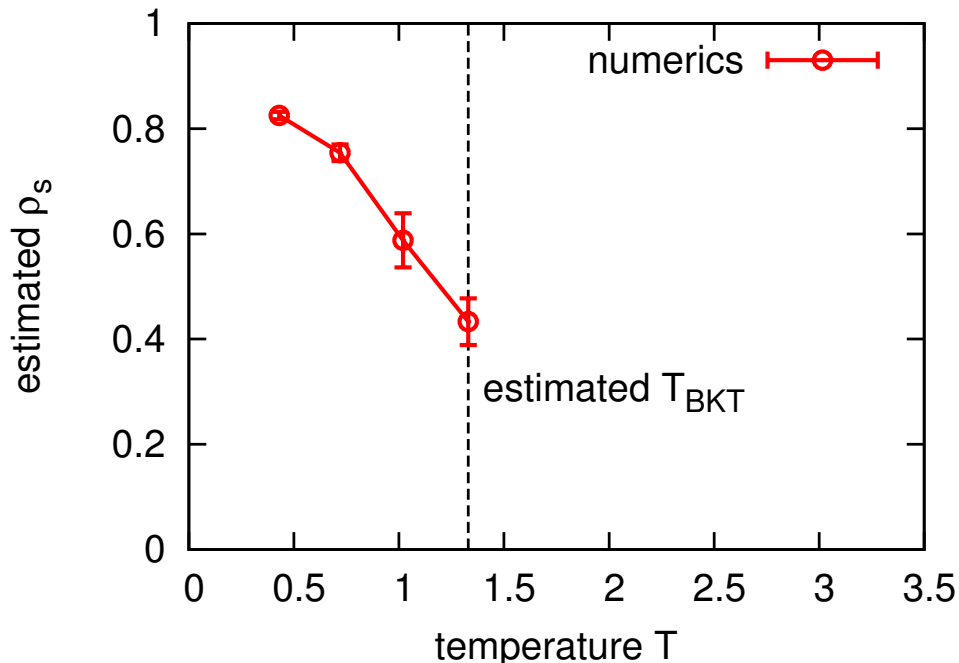


FIG. 8. (Color online) Estimated superfluid fraction  $\rho_s$  with respect to different values of temperature. The superfluid fraction is evaluated by fitting the power-law exponent in Fig. 7 and inverting the second relation in equation (42).

A “plasma” of tightly placed “ghost” vortices is simply a null set of a weakly nonlinear dispersive wave field. There is no closed description of such a field in terms of the vortices only. In particular, the log-like expression for the vortex energy used in the physical BKT argument (reproduced in section VI)) would be invalid in this case. Instead, a more fundamental physical quantity in this case is the wave spectrum, evolution of which satisfies the kinetic equation (13).

Figure 12 shows 2D frames in the physical space with positive and negative vortices taken from simulations with  $L = 256$ ,  $\bar{\rho} = 1$  and different  $\epsilon_2$  (temperatures). Figure 13 shows a plot of the number of vortices as a function of  $\epsilon_2$  in the same simulations. As expected, we see that the number of vortices is decreased when the system is cooled, and indeed we see formation of vortex dipoles at low  $T$ . However, this transition is not sharp, and the dipoles are dominant only for temperatures which are significantly lower than  $T_{BKT}$  (see the frame corresponding to  $\epsilon_2 \approx T = 0.5$  in Figure 12)). For  $T \lesssim T_{BKT} \approx 1.39$  the dipoles are in minority: for  $\epsilon_2 \approx T = 1.07$  we see, apart from several dipoles, several remaining isolated

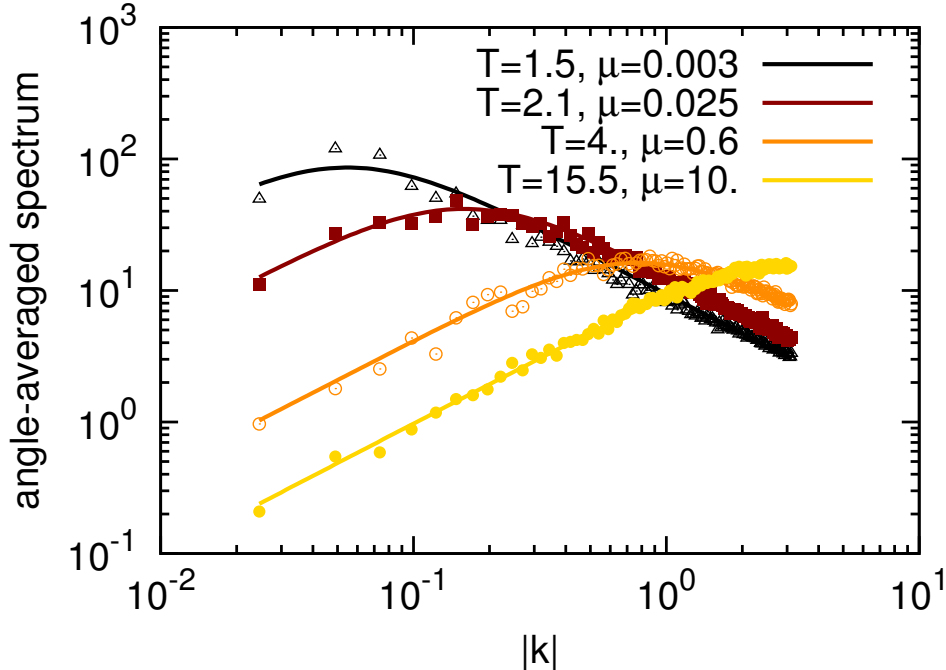


FIG. 9. (Color online) Steady state spectra in high-energy simulations with absent condensate. The fitted curves correspond to the Rayleigh-Jeans distribution (16) integrated over angles, that is  $N_k = \int_0^{2\pi} n_k k d\theta$ . Results taken from simulations with  $L = 256$ .

vortices as well as some clusters of positive and negative vortices of larger sizes, with three or more vortices in them. In fact, vortex clusters are seen also for  $T \gtrsim T_{BKT}$ , eg. for  $\epsilon_2 \approx T = 1.52$  and even for  $\epsilon_2 \approx T = 2.06$ . As far as we know such a phenomenon of vortex clustering has never been discussed in the context of the BKT transition, and its possible dynamical role is yet to be understood.

It is clear, however, that most vortices, in pairs, in clusters or in a vortex “plasma”, are not separated by distances larger than  $\xi$ . Watching them in dynamics on a video reveals that these vortices sporadically flicker in and out of existence rather than get engaged in a hydrodynamic type of motion (see movies in supplementary material). Thus, these are ghost vortices representing short-wave fluctuations of a weakly nonlinear wave field, (waves for the high  $T$  regime, Bogoliubov excitations in the low  $T$  regime), and their description in terms of the hydrodynamic Hamiltonian is invalid. With these conclusions, it becomes even more puzzling why the physical argument based on the hydrodynamic Hamiltonian lead to an accurate BKT prediction for the power-law decay of correlations with the near-transition

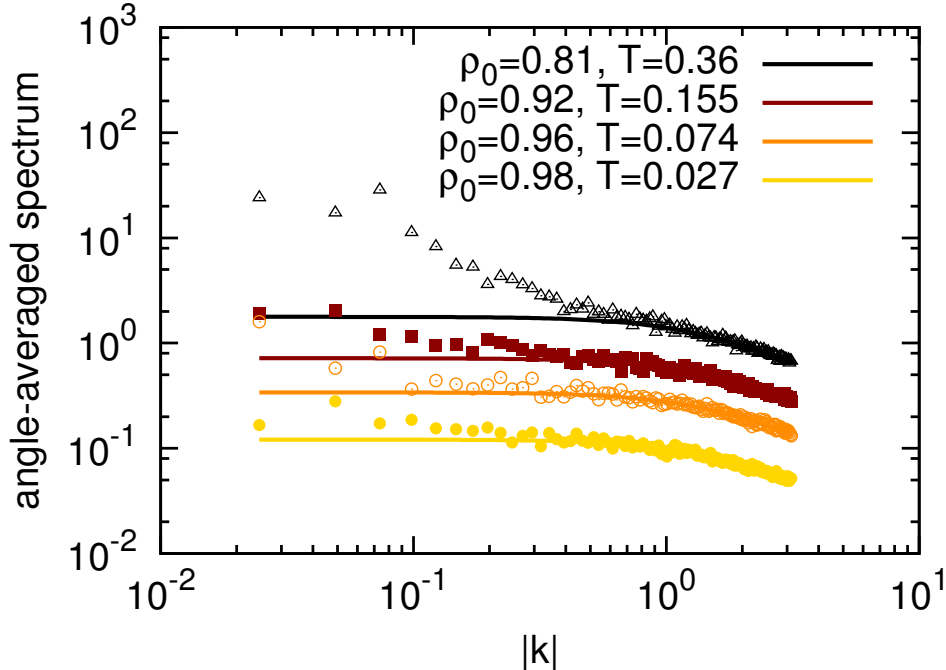


FIG. 10. (Color online) Low-energy cases with strong condensate levels. Spectra of the Bogoliubov normal variables (21). The fitted curves correspond to the Rayleigh-Jeans distribution (30) integrated over angles, that is  $N_k = \int_0^{2\pi} n_k k d\theta$ . Results taken from simulations with  $L = 256$ .

exponent  $\alpha = 1/4$ .

## VIII. CONCLUSIONS

In this paper, we studied statistical equilibria in 2D NLS model which is truncated in the Fourier space. No forcing or dissipation was introduced; we let the nonlinearity do phase-space mixing and bringing the system to thermodynamic equilibrium. Our goal was to study the physical processes associated with random interacting waves and vortices which accompany the Bose-Einstein condensation and the BKT transition and examine feasibility of the standard physical assumptions put into derivation of the power-law correlations and the BKT transition.

Because the NLS equation is also a universal model widely used in Wave Turbulence (WT), we would like to establish closer links of the condensed matter theory of the above phenomena with the WT approach and interpretations. Our choice of fully conservative formulation allowed us to look at the nonlinear dynamics of waves and vortices in their

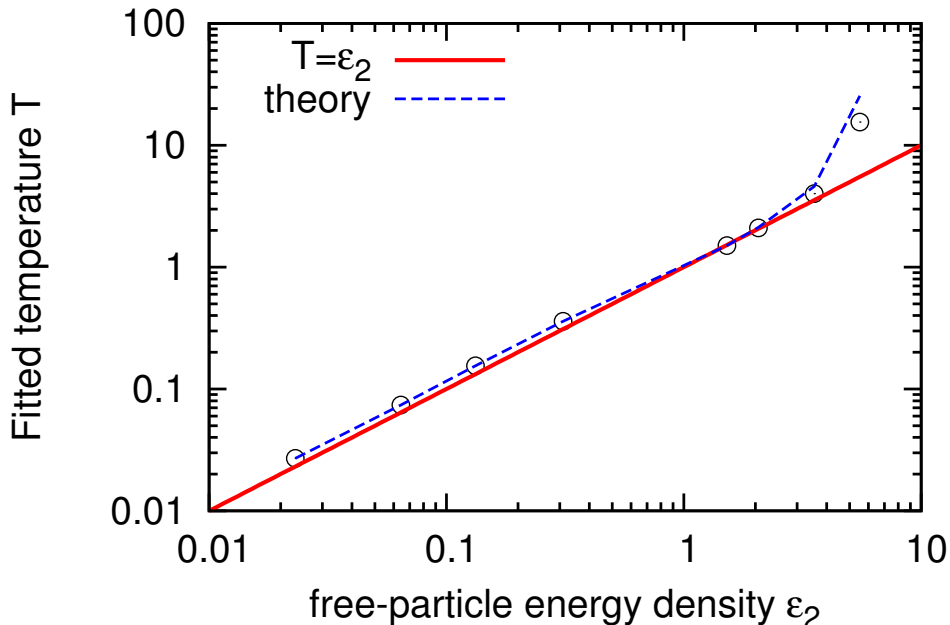


FIG. 11. (Color online) Temperatures evaluated by fitting with the Bogoliubov or the Rayleigh-Jeans dispersions in the corresponding regimes. The straight line correspond  $T = \epsilon_2$ . The dashed line correspond to prediction (17). Results taken from simulations with  $L = 256$ .

purity and unobstructed by external stochasticity associated with a thermal bath. In this respect our approach is different from the one of Ref [25] where a thermal bath was added to the model.

Our numerical results support the view that the 2D NLS system in thermal equilibrium represents a four-wave weak WT (described by the kinetic equation (13)) at high temperatures and a three-wave weak WT (described by the kinetic equation (27)) at low temperatures. Weakness of WT was confirmed using  $(k, \omega)$ -plots where it manifested itself as narrow distributions around the linear-wave dispersion curves. Importantly, not only the exponential decay of correlations at high  $T$ , but also the power-law decay at low  $T$  can be described within the WT approach. For that WT has to be reformulated at low  $T$  using the hydrodynamic formulation, which allows to use WT in cases where the phase experiences order one or greater changes.

At the intermediate temperatures, i.e. the range in which the condensation and the BKT transition occur, the system can be viewed as strong turbulence in which the linear and the

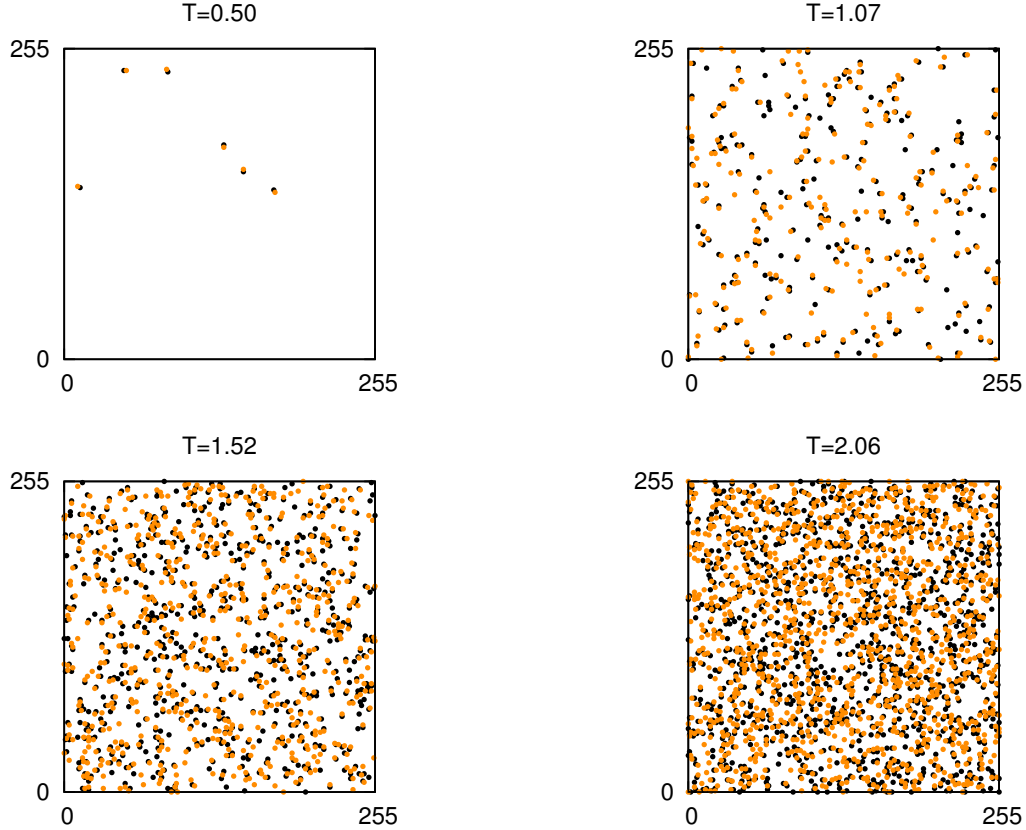


FIG. 12. (Color online) Quantum vortices in statistical steady state in simulations with  $L = 256$ . Clockwise and anti-clockwise vortices are shown by blue and red colours respectively.

nonlinear effects balance. In fact, it is precisely the balance of the linear and the nonlinear terms in the NLS equation that appears to give the correct criterion for the condensation and the BKT transition, and the respective transition temperatures can be found from this condition. To be precise, we found that for the same system size ( $L = 256$ ) the condensation temperature  $T_c$  is, within the error bar, the same as  $T_{BKT} \approx 1.39$ , and that this temperature corresponds to the ratio of the interaction and the free-particle energies  $\approx 0.5$ .

We have found some striking confirmations of the predictions of the power-law correlation decay and of its exponent at the BKT transition temperature,  $\alpha = 1/4$ , as well as a reasonable agreement with the prediction of the relation between the superfluid density and the transition temperature,  $T_{BKT} = \pi\rho_s$ . Moreover, we observed that the superfluid density  $\rho_s$  does not depend on the system size  $L$  and the condensate fraction  $\rho_0$  scales like a power-law with respect to  $L$  above the BKT transition.

At the same time, we found inconsistency of the basic physical assumptions used for

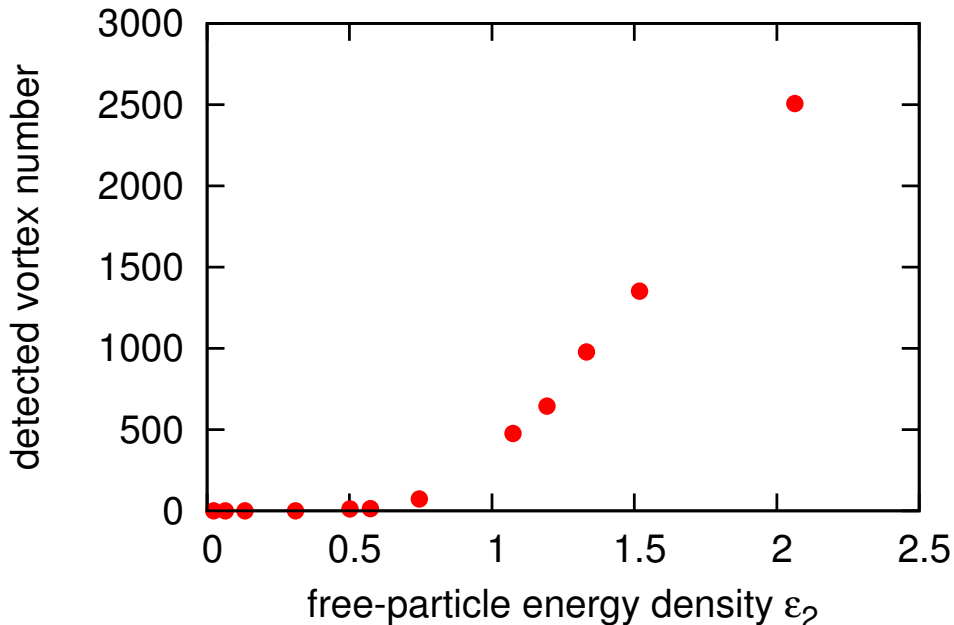


FIG. 13. (Color online) Measured number of vortices in the system for different values of linear energy. Results taken from simulations having side equal to  $L = 256$ .

deriving the power-law correlations near the BKT transition temperatures (i.e. postulating the superfluid density and thereby redefining the hydrodynamic and Bogoliubov approach) as well as the BKT threshold (i.e. using the picture of hydrodynamic vortices with log-like expressions for their energies). First, the frequency shifts for  $k \rightarrow 0$  obtained from the  $(k, \omega)$ -plots contradict the naive view that for intermediate temperatures the system can be described by Bogoliubov approach with some effective superfluid density. Second, at the BKT transition temperature (as well as well below and above it) the NLS vortices have properties very different from their hydrodynamic counterparts and there is no closed description of the system in terms of these vortices only. The vortices are not separated by distances  $> \xi$  sufficient for them to become self-sustained and hydrodynamic-like. Also, the physical picture that at crossing  $T_{BKT}$  the system changes from being a plasma of individual vortices to a gas of bound vortex dipoles appears to be oversimplified. The transition appears to be rather gradual and in a wide range of temperatures around  $T_{BKT}$  one observes vortex clusters. The mean size of such vortex clusters gradually decreases at  $T$  is decreased, and only of temperatures significantly lower than  $T_{BKT}$  vortex dipoles start to dominate. However, quite small further decrease of  $T$  leads to disappearance of vortices

altogether.

It is often said that more rigorous and systematic description of the BKT transition exists within the renormalization group approach. However, as we can see from the present paper, more work remains to be done for understanding the underlying physical properties in terms of interacting waves, vortices and or/and other nonlinear hydrodynamic structures.

## ACKNOWLEDGMENTS

Authors wish to express their gratitude to C.F. Barenghi, D. Gangardt, N. Proukakis, H. Salman, and Y. Sergeev for interesting discussions and suggestions.

- 
- [1] L. Pitaevskii and S. Stringari, *Bose-Einstein Condensation*, International Series of Monographs on Physics (Clarendon Press, 2003) ISBN 9780198507192.
  - [2] N. D. Mermin and H. Wagner, *Physical Review Letters*, **17**, 1133 (1966).
  - [3] N. N. Bogoliubov and N. N. Bogoliubov (Jr.), *Introduction to Quantum Statistical Mechanics* (2nd ed., World Scientific, Singapore, 2009).
  - [4] V. Berezinskii, *Sov. Phys. JETP*, **32**, 493 (1971).
  - [5] J. M. Kosterlitz and D. J. Thouless, *Journal of Physics C Solid State Physics*, **6**, 1181 (1973).
  - [6] J. Kosterlitz, *Journal of Physics C: Solid State Physics*, **7**, 1046 (1974).
  - [7] S. Nazarenko, *Wave turbulence* (Springer-Verlag, 2011).
  - [8] A. Dyachenko, A. Newell, A. Pushkarev, and V. Zakharov, *Physica D*, **57**, 96 (1992).
  - [9] V. E. Zakharov and S. V. Nazarenko, *Physica D: Nonlinear Phenomena*, **201**, 203 (2005), ISSN 0167-2789.
  - [10] Y. Lvov, S. Nazarenko, and R. West, *Physica D: Nonlinear Phenomena*, **184**, 333 (2003), ISSN 0167-2789.
  - [11] S. Nazarenko and M. Onorato, *Physica D: Nonlinear Phenomena*, **219**, 1 (2006), ISSN 0167-2789.
  - [12] S. Nazarenko and M. Onorato, *Journal of Low Temperature Physics*, **146**, 31 (2007), ISSN 0022-2291.
  - [13] C. Connaughton, C. Josserand, A. Picozzi, Y. Pomeau, and S. Rica, *Phys. Rev. Lett.*, **95**,

- 263901 (2005).
- [14] G. Düring, A. Picozzi, and S. Rica, *Physica D: Nonlinear Phenomena*, **238**, 1524 (2009), ISSN 0167-2789.
- [15] N. Vladimirova, S. Derevyanko, and G. Falkovich, *Phys. Rev. E*, **85**, 010101 (2012).
- [16] N. Berloff and B. Svistunov, *Physical Review A*, **66**, 13603 (2002).
- [17] D. Proment, S. Nazarenko, and M. Onorato, *Special Issue on Small Scale Turbulence*, *Physica D: Nonlinear Phenomena*, **241**, 304 (2012).
- [18] G. Krstulovic and M. Brachet, *Phys. Rev. E*, **83**, 066311 (2011).
- [19] J. Schole, B. Nowak, and T. Gasenzer, *Phys. Rev. A*, **86**, 013624 (2012).
- [20] C. Sun, S. Jia, C. Barsi, S. Rica, A. Picozzi, and J. W. Fleischer, *Nature Physics*, **8**, 471 (2012).
- [21] V. Shukla, M. Brachet, and R. Pandit, ArXiv e-prints (2013), arXiv:1301.3383 [nlin.CD].
- [22] Z. Hadzibabic and J. Dalibard, *Rivista del Nuovo Cimento*, **34**, 389 (2011).
- [23] J. B. Kogut, *Rev. Mod. Phys.*, **51**, 659 (1979).
- [24] S. W. Pierson, *Philosophical Magazine Part B*, **76**, 715 (1997), <http://www.tandfonline.com/doi/pdf/10.1080/01418639708241138>.
- [25] C. J. Foster, P. B. Blakie, and M. J. Davis, *Phys. Rev. A*, **81**, 023623 (2010).
- [26] V. Zakharov, S. Musher, and A. Rubenchik, *Phys. Rep.*, **129**, 285 (1985).
- [27] V. Zakharov, V. L'vov, and G. Falkovich, *Kolmogorov Spectra of Turbulence 1: Wave Turbulence* (Springer-Verlag, 1992).
- [28] V. Popov, *Functional Integrals in Quantum Field Theory and Statistical Physics* (Reidel, Dordrecht, 1983).
- [29] S. Nazarenko and R. West, *Journal of Low Temperature Physics*, **132**, 1 (2003), ISSN 0022-2291.
- [30] N. Prokof'ev, O. Ruebenacker, and B. Svistunov, *Phys. Rev. Lett.*, **87**, 270402 (2001).